Research Article

Journal of Environmental Nanotechnology

# Creation of Ultra-long Pure Magnetization Needle by Circularly Polarized Beam with a Ternary Optical Element

M. Udhayakumar, Haresh M. Pandya, K. B. Rajesh*

*Department of Physics, Chikkanna Government Arts College, Tiruppur, TN, India*

Received: 21.08.2019 Accepted: 25.09.2019 Published: 30-09-2019

*rajeshkb@gmail.com

## ABSTRACT

The light-induced magnetization needle was made by tightly focusing a circularly polarized beam and modulating it using a self-designed ternary hybrid (phase/amplitude) filter (THF), based on Vector diffraction theory and the Inverse Faraday effect. The adaptable particle swarm optimization (PSO) searching technique prudently optimized the phase and amplitude patterns of THF. It was noted that optimizing produced an ultra-long pure magnetization needle with a lateral sub-wavelength scale and a super-long spherical magnetization chain with three-dimensional super-resolution. The present research on super-resolution magnetization patterns is very valuable in high density all-optical magnetic recording, atomic trapping and confocal and magnetic resonance imaging.

**Keywords:** Azimuthally polarized beam; Diffractive optical element; Super-resolution.

## 1. INTRODUCTION

Due to its potential applications in all-optical magnetic recording (AOMR) (Stanciu *et al.* 2007; Khorsand *et al.* 2012; Mangin *et al.* 2014), confocal and magnetic resonance microscopy (Grinolds *et al.* 2014), atom trapping (Vetsch *et al.* 2010; Schneeweiss *et al.* 2014) and multi-dimensional magneto-optical data storage (Zijlstra *et al.* 2009; Gu *et al.* 2014), the ultra-fast response of the light-induced magnetization field in the magneto-optical film has piqued the interest of researchers in the last year. All of these applications require a pure longitudinal magnetization focus structure that allows for a well-defined magnetization direction in the material on an ultra-small 3D volume beyond the diffraction limit ($\sim\lambda^3/8$). For applications such as high-density magnetic-optical data storage and high-resolution magnetic resonance imaging, a magnetization focused structure of this sort is essential. Furthermore, multiple magnetic particle trapping and manipulation need spherical 3D super-resolution spot multiple into an array, which is necessary to enhance the processing speed and power efficiency of magneto-optical recording. Many attempts have been made to modify the magnetization structure by controlling the mutual interaction between the polarisation singularities of a cylindrical polarisation beam and an optical vortex (Jiang *et al.* 2013; Qin *et al.* 2015; Gong *et al.* 2016; Yan *et al.* 2017; Sicong Wang *et al.* 2018), in conjunction with amplitude/phase modulation (Wang *et al.* 2014; Nie *et al.* 2015; Ma *et al.* 2015; Yan *et al.* 2017a, 2017b; Udhayakumar *et al.* 2018a; 2018b). A tightly focused circularly polarized beam with a high numerical aperture objective has been suggested as an effective way to induce and reverse longitudinal magnetization in the magnetic material when the handedness of a circularly polarized beam is modified (Savoini *et al.* 2012; El Hadri *et al.* 2016a, 2016b, 2017; Pierre Vallobra *et al.* 2017; Quessab *et al.* 2018). Recently, the Particle swarm optimization (PSO) algorithm, which is inspired by the emergent motion of a flock of birds hunting for food, has become a powerful tool to determine the parameters of DOEs for improving the performances of optical fields (Jie Lin *et al.* 2016; Mohamed Ahmed Mohandes, 2012). It is manifested that the PSO performs well in finding a good solution to optimize the objective function. In contrast to other optimization techniques, the PSO has better search performance with faster and more stable convergence rates (Ioan Cristian Trelea, 2003). Although this novel optimization scheme has several merits, such as global optimization, fast convergence and reduced iteration number, combining both the generic algorithm and PSO algorithm will make the whole optimization system more complex (Jie Lin *et al.* 2016; Mohamed Ahmed Mohandes, 2012). In this work, the ability of producing a highly contained magnetic field reaching up to 10.2 with no side lobes and an extremely low transverse magnetization component has been numerically demonstrated, based on VDT and IFE. The magnetization spots that were stretched axially by a self-designed ternary hybrid (phase/amplitude) filter

(THF) and focused on a high NA objective using a circularly polarized annular multi-Gaussian beam were also shown.

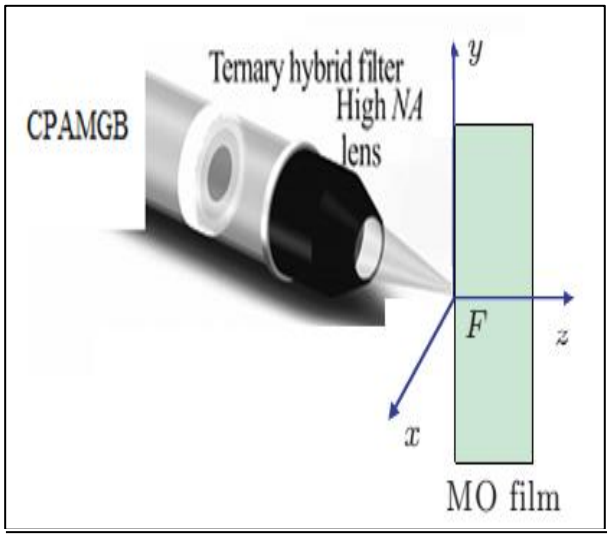


**Fig. 1: Schematic set-up for generating pure longitudinal magnetization needle using circularly polarized annular multi-Gaussian beam (CPAMGB) with THF**

## 2. THEORY

The schematic of the proposed method is shown in Fig. 1. In a tight focusing system, the amplitude of the multi-Gaussian beam at the entrance plane ($z_0$=0), in the cylindrical coordinate system (ρ, φ, z0), can be written as (Jian-Nong *et al.* 2011),

$$P(\theta)=\left(\frac{\theta}{\theta_0}\right)^m \sum_{n=-N}^{N} \exp\left[-\left(\frac{\theta-\theta_c-n\omega_0}{\omega_0}\right)^2\right] \qquad (1)$$

Here, $\theta$ is the converging semi-angle. $\theta_{max}$ is the maximum converging semi-angle, which is related to objective numerical aperture by, $\theta_{max}= arcsin(NA)$. $\theta_0$ is an angle which, along with integer $m$, determines the shape of the modulation function. $\theta_0$ is usually chosen to be slightly smaller than $\theta_{max}$. $\theta_c$ determines the radial position translation of $P(\theta)$. Here we take $\theta_c = \theta_{max}/2$. $w_0$ is the waist width of a single Gaussian beam, which is calculated by the formula,

$$w_0 = 1/2 \times \frac{\theta \max}{N+\left\{1-\ln\left[\sum_{n=-N}^{N}\exp(-n^2)\right]\right\}^{1/2}} \qquad (2)$$

Equation (1) describes an object beam. It is suitable to convert Eq. (1) from a function of angle into a function of radial polar coordinate. One may substitute $\theta$ with arcsin $(r/f)$, where $f$ is the focal distance of the objective. In Eq. (1), the factor $(\theta/\theta_0)$ measures that most of the light energy is located on the annular edge of the pupil. More energy is focused in the annular edge area where the converging semi-angle is larger than $\theta_0$ when the integer $m$ is increased. The annular multi-Gaussian beam's amplitude is dramatically lowered as it approaches the pupil's outer border due to the sum of (2N + 1) spatially uniformly dispersed Gaussian beams. An amplitude-modulated beam may be created by programming an appropriate phase mask on the spatial light modulator. Based on Richards and Wolf's vectorial diffraction method widely used for high NA focusing systems at arbitrary incident polarization (Richards and Wolf, 1959), the electric field E (ρ, ϕ, z) in the vicinity of the focal region of an incident circularly polarized beam can be written as,

$$E_{cir}^{L}(\rho_c,\phi_c,z_c)=\begin{bmatrix} ie_x+e'_x \\ ie_y+e'_y \\ ie_z+e'_z \end{bmatrix}=\begin{bmatrix} A(T_0+T_2e^{-i2\phi_c}) \\ -iA(T_0-T_2e^{-i2\phi_c}) \\ -2iAT_1e^{-i2\phi_c} \end{bmatrix} \qquad (3)$$

where,

$$T_0=\int_0^{\alpha}(1+\cos\theta)\sqrt{\cos\theta}P(\theta)\,A(\theta)\sin\theta J_0(k\rho_c\sin\theta)\exp(ikz_c\cos\theta)d\theta$$

$$T_1=\int_0^{\alpha}\sin^2\theta\sqrt{\cos\theta}P(\theta)\,A(\theta)J_1(k\rho_c\sin\theta)\exp(ikz_c\cos\theta)d\theta \qquad (4)$$

$$T_2=\int_0^{\alpha}(1-\cos\theta)\sqrt{\cos\theta}P(\theta)\,A(\theta)\sin\theta J_2(k\rho_c\sin\theta)\exp(ikz_c\cos\theta)d\theta$$

Here, α is the convergence semi-angle of the lens, k=2π/λ is the wavenumber, A is a constant, and $J_n$ is the $n^{th}$ Bessel function of the first kind. The magnetization can be induced by the inverse Faraday effect. For simplicity, the conducting electrons in the magneto-optical film can be treated as a collision-less plasma in which the electrons can move freely, at least on the time scale given by the period of the high-frequency field and the wave's fluctuating magnetic field is neglected. Thus, the magnetization M generated in the plasma by the high-frequency field is proportional to $iE\times E^*$ (Van der Ziel *et al.* 1965), which can be expressed as (Hertel, 2006; Volkov and Novikov, 2002)

$$M(\rho_c, \phi_c, z_c) = i\gamma E \times E^* \qquad (5)$$

where, γ is a magneto-optical constant. Substituting Eq. (3-4) into Eq. (5), we obtain the magnetization $M_n$ normalized to $\gamma$ and for the incident left-handed circularly polarized light that is given by,

$$M_n^L(\rho_c, \phi_c, 0) = \frac{M_n^L(\rho_c, \phi_c, 0)}{\gamma A}\begin{bmatrix} -4T_1(T_0 + T_2\sin\phi_c) \\ 4T_1(T_0 + T_2\cos\phi_c) \\ -2(T_0^2 - T_2^2) \end{bmatrix} \qquad (6)$$

From Eqs. (6), one can immediately see that the magnetization is a three-dimensional distribution in general.

## 3. NUMERICAL SIMULATION RESULTS AND DISCUSSION

The fixed parameters used for the calculations are λ = 1 and NA = 0.85. Here, for simplicity, it has been assumed that the refractive index n = 1 and order ($m$) of CPAMGB is 30. For all calculations in length, the unit is normalized to λ and the energy density is normalized to unity. Fig. 2 (a) shows the 2D magnetization distribution obtained for the incident CPAMGB with $m$ = 30. Fig. 2 (b) and (c) show the corresponding magnetization distribution in the radial and axial planes. From Fig. 2(b) and (c), it has been noted that the FWHM of the magnetization spots was 0.45λ and its focal depth was 8λ. Moreover, the residual radial magnetization distribution is only 10% of the longitudinal distribution and there were no side lobes observed. Hence such a magnetization spot can be utilized for all-optical helical switching.

However, improving the focal depth of the magnetization point without increasing the spot size is critical. However, for helical depended switching, the incident beam should be circularly polarized, and the authors have demonstrated the possibility of creating the super-long magnetization needle of sub-wavelength scale magnetization spots using a novel sine-shaped ternary hybrid filter (THF), well-devised with the modified PSO algorithm to produce a pure longitudinally magnetization needle with ultra-long DOF by strongly focused circularly polarized annular multi-Gaussian beam (CPAMGB).

$$A(\theta) = \sum_{i=0}^{m} p_i \sin(2\pi s_i / \alpha)$$

is the transmittance function with $p_i$, $s_i$ and $m$ being the radius and phase factors and the belt number of the-THFs (Xiaoyu Weng *et al.* 2014). It should be mentioned that it was different from the common binary DOE, and one can controllably vary the amplitude (0-1) and the phase (0/π) of THF. Moreover, the proposed PSO algorithm can robustly solve the multiple parameters of the THF with fast convergence and global optimum.

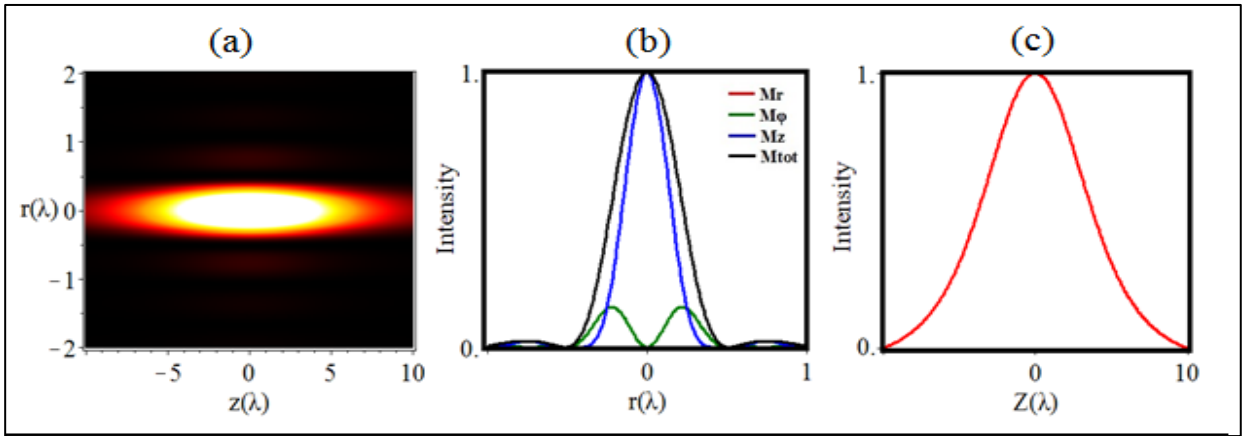


**Fig. 2: (a) 2D Normalized magnetization distribution in $r-z$ plane for circularly polarized annular multi-Gaussian beams ($m$ = 30) (b) Normalized magnetization profiles along the radial direction at $z$ = 0 and (c) Magnetization profiles along the $z$-axis at $r$ = 0**

**Table 1. Parameters of the sine-shaped ternary hybrid filter for $m = 2$**

| Order of belts | First | Second | Third |
|---|---|---|---|
| Normalized transmittance | 1.024 | 2.041 | 3.070 |
| Phase parameter | 1 | 0.183 | 0.278 |
| Amplitude parameter | 0.725 | 1.216 | 1.158 |

Fig. 3 (b) has shown that the FWHM of the generated magnetic probe was 0.4λ. The on axial intensity distribution shown in Fig. 3 (c) revealed that the generated magnetization focal segment was axially homogenous, and its FWHM the DOF was around 6.4λ. Thus by using a single focusing unit and properly axial field, strength was achieved in the focal region. The perfect magnetization needle and the simple approach provided a roadmap for ultrahigh density magnetic storage, magnetic lattice fabrication for spin-wave operation and atomic trapping.

Fig. 4 (a) has shown the 2D magnetization distribution obtained for the incident CPAMGB with $m$ = 30. It was noted from Fig. 4 (b) that the FWHM of generated magnetization spot was only 0.4λ with no side lobe and the residual transverse magnetization was still 5% of the longitudinal magnetization distribution. It was noted from Fig. 4(c) that the depth of focus (DOF) of the generated magnetization spot very well extended up to 10.2λ. Moreover, since the HGPSO combines the genetic algorithm, self-adaptive parameters, recombination and mutation operation (Jie Lin *et al.* 2016), the program structure of the HGPSO is more complex than that of PSO, thus leading to low optimization search efficiency in multi-dimensional data optimization. In these aspects, the proposed PSO is a feasible and efficient way to design and optimize the filters for achieving the magnetization needle. This type of sub-wavelength size needle of longitudinal magnetization point has applications in ultrahigh density magnetic storage, magnetic lattice fabrication for spin-wave operation and atomic trapping.

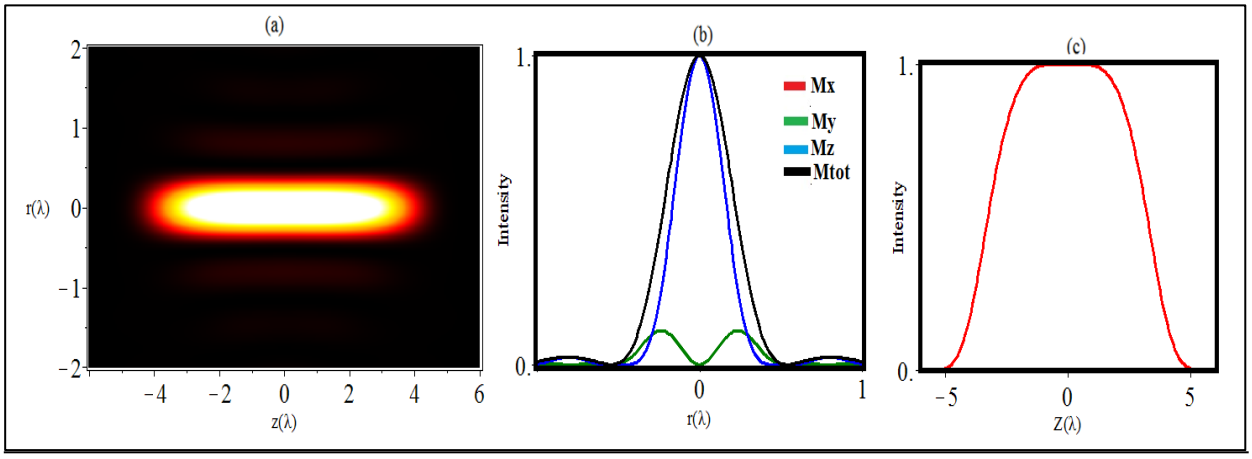


**Fig. 3: (a) 2D Normalized super-long magnetization needle with well-axial homogeneity ($m = 2$) (b) Normalized magnetization profiles along the radial direction at $z = 0$ and (c) Magnetization profiles along $z$-axis at $r = 0$**

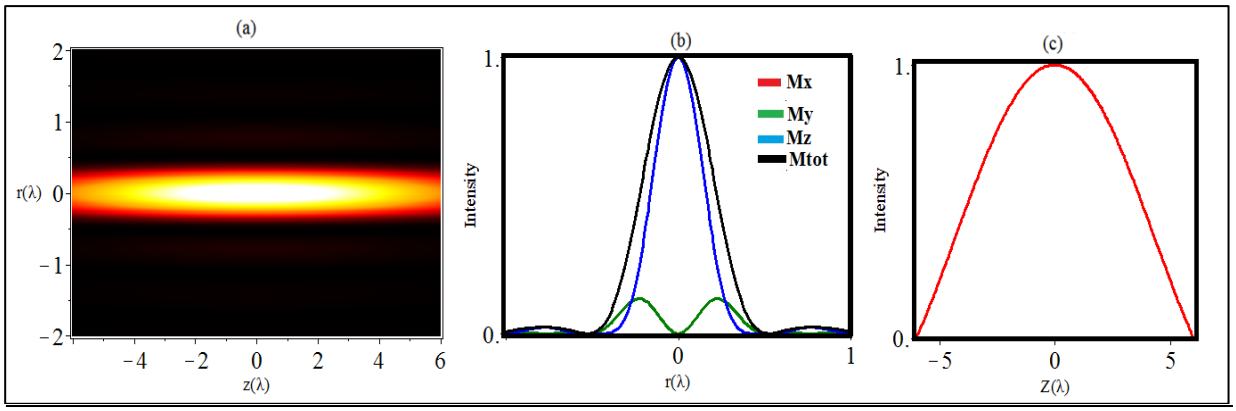


**Fig. 4: (a) 2D Normalized magnetization needle for circularly polarized annular multi-Gaussian beams with THF, when $m$ = 30 (b) Normalized magnetization profiles along the radial direction at $z$ = 0 and (c) Magnetization profiles along $z$-axis at $r$ = 0**

## 4. CONCLUSION

The light-induced magnetization needle was formed utilising Vector diffraction theory and the Inverse Faraday effect by tightly concentrating a circularly polarised annular multi-Gaussian beam modulated by a self-designed ternary hybrid (phase/amplitude) filter (THF). The adaptable particle swarm optimization (PSO) searching technique prudently optimised the phase and amplitude patterns of THF. It was stated that by optimising sine-shaped THFs to construct an ultra-long pure magnetization needle with lateral sub-wavelength scale, a magnetization needle with FWHM of 0.4λ and DOF of 10.2λ was obtained. The ultrahigh density all-optical magnetic recording needle with a super high aspect ratio and strong axial homogeneity, as well as producing magnetic lattices for spin-wave operation and atomic trapping with flexibility has been produced.

## FUNDING

This research received no specific grant from any funding agency in the public, commercial, or not-for-profit sectors.

## CONFLICTS OF INTEREST

The authors declare that there is no conflict of interest.

## COPYRIGHT



## REFERENCES

El Hadri, M. S., Michel Hehn, Philipp Pirro, Charles-Henri Lambert, Grégory Malinowski, Eric E. Fullerton and Stéphane Mangin, Domain size criterion for the observation of all-optical helicity-dependent switching in magnetic thin films, *Phys. Rev. B.*, 94(6), 064419 (2016b). https://dx.doi.org/10.1103/PhysRevB.94.064419

El Hadri, M. S., Pirro, P., Lambert, C.-H., Bergeard, N., Petit-Watelot, S., Hehn, M., Malinowski, G., Montaigne, F., Quessab, Y., Medapalli, R., Fullerton, E. E. and Mangin, S., Electrical characterization of all-optical helicity-dependent switching in ferromagnetic Hall crosses, *Appl. Phys. Lett.*, 108, 092405-5 (2016a). https://dx.doi.org/10.1063/1.4943107

Gong, L., Wang, L., Zhu, Z., Wang, X., Zhao, H. and Gu, B., Generation and manipulation of super-resolution spherical magnetization chains, *Appl. Opt.*, 55(21), 5783–5789 (2016). https://dx.doi.org/10.1364/AO.55.005783

Grinolds, M. S., Warner, M., De Greve, K., Dovzhenko, Y., Thiel, L., Walsworth, R. L., Hong, S., Maletinsky, P. and Yacoby, A., Subnanometre resolution in three-dimensional magnetic resonance imaging of individual dark spins, *Nat Nanotechnol.*, 9(4), 279-284 (2014). https://dx.doi.org/10.1038/nnano.2014.30.

Gu, M., Xiangping Li and Yaoyu Cao, Optical storage arrays: a perspective for future big data storage, *Light: Sci. Appl.*, 3, e177 (2014). https://dx.doi.org/10.1038/lsa.2014.58

Hadri, M. S., Hehn Michel, Malinowski Gregory, Mangin Stephane, Materials and devices for all-optical helicity-dependent switching, *J. Phys. D: Appl. Phys.*, 50(13), 133002 (2017). https://dx.doi.org/10.1088/1361-6463/aa5adf

Hertel, R., Theory of the inverse Faraday Effect in metals, *J. Magn. Magn. Mater*., 303(1), L1–L4 (2006). https://dx.doi.org/10.1016/j.jmmm.2005.10.225

Ioan Cristian Trelea, The particle swarm optimization algorithm: convergence analysis and parameter selection, *Inf. Process. Lett.*, 85(6), 317-325 (2003). https://dx.doi.org/10.1016/S0020-0190(02)00447-7

Jiang, Y., Li, X. and Gu, M., Generation of sub-diffraction-limited pure longitudinal magnetization by the inverse Faraday effect by tightly focusing an azimuthally polarized vortex beam, *Opt. Lett*., 38(16), 2957–2960 (2013). https://dx.doi.org/10.1364/OL.38.002957

Jian-Nong, C., Qin-Feng, X. and Gang, W., Tight focus of a radially polarized and amplitude-modulated annular multi-Gaussian beam, *Chin. Phys., B20*, 114211 (2011). https://dx.doi.org/10.1088/1674-1056/20/11/114211

Jie Lin, Hong-yang Zhao, Yuan Ma, Jiubin Tan and Peng Jin, New hybrid genetic particle swarm optimization algorithm to design multi-zone binary filter, *Opt. Express*, 24(10), 10748-10758 (2016). https://dx.doi.org/10.1364/OE.24.010748

Khorsand, A. R., Savoini, M., Kirilyuk, A., Kimel, A. V., Tsukamoto, A., Itoh, A. and Rasing, Th., Role of magnetic circular dichroism in all-optical magnetic recording, *Phys. Rev. Lett.*, 108(12), 127205 (2012). https://dx.doi.org/10.1103/PhysRevLett.108.127205

Ma, W., Zhang, D., Zhu, L. and Chen, J., Super-long longitudinal magnetization needle generated by focusing an azimuthally polarized and phase-modulated beam, *Chin. Opt. Lett.*, 13(5), 52101–52105 (2015).

Mangin, S., Gottwald, M., Lambert, C., Steil, D., Uhlř, V., Pang, L., Hehn, M., Alebrand, S., Cinchetti, M., Malinowski, G., Fainman, Y., Aeschlimann, M. and Fullerton, E. E., Engineered materials for all-optical helicity-dependent magnetic switching, *Nat. Mater*., 13, 286–292 (2014). https://dx.doi.org/10.1038/nmat3864

Mohamed Ahmed Mohandes, Modeling global solar radiation using partiticle swarm optimization (PSO), Solar Energy, 86(11), 3137-3145 (2012). https://dx.doi.org/10.1016/j.solener.2012.08.005

Nie, Z., Ding, W., Shi, G., Li, D., Zhang, X., Wang, Y. and Song, Y., Achievement and steering of light-induced sub-wavelength longitudinal magnetization chain, *Opt. Express*, 23(16), 21296–21305 (2015). https://dx.doi.org/10.1364/OE.23.021296

Pierre Vallobra, Thibaud Fache, Yong Xu, Lei Zhang, Gregory Malinowski, Michel Hehn, Juan-Carlos Rojas-Sánchez Eric.E. Fullerton and Stephane Mangin, Manipulating exchange bias using all-optical helicity-dependent switching, *Phys. Rev. B.*, 96, 144403 (2017).

Qin, F., Huang, K., Wu, J., Jiao, J., Luo, X., Qiu, C. and Hong, M., Shaping a subwavelength needle with ultra-long focal length by focusing azimuthally polarized light, *Sci. Rep*., 5, 9977 (2015). https://dx.doi.org/10.1038/srep09977.

Quessab, Y., Medapalli, R., El Hadri, M. S., Hehn, M., Malinowski, G., Fullerton, E. E. and Mangin, S., Helicity-dependent all-optical domain wall motion in ferromagnetic thin films, *Phys. Rev. B*., 97(5), 054419 (2018). https://dx.doi.org/10.1103/PhysRevB.97.054419

Richards, B. and Wolf, E., Electromagnetic diffraction in optical systems, II. Structure of the image field in an aplanatic system, *Proc. Roy. Soc. A.*, 253, 358–379 (1959). https://dx.doi.org/10.1098/rspa.1959.0200

Savoini, M., Medapalli, R., Koene, B., Khorsand, A. A., Le Guyader, L., Duo, L., Finazzi, M., Tsukamoto, A., Itoh, A., Nolting, F., Kirilyuk, A., Kimel, A. V. and Rasig, Th., Highly efficient all-optical switching of magnetization in GdFeCo microstructures by interference-enhanced absorption of light, *Phys. Rev. B.*, 86, 140404(R) (2012). https://dx.doi.org/10.1103/PhysRevB.86.140404

Schneeweiss, P., Le Kien, F. and Rauschenbeutel, A., Nanofiber-based atom trap created by Combining fictitious and real magnetic fields, *New J. Phys.*, 16, 013014 (2014). https://dx.doi.org/10.1088/1367-2630/16/1/013014

Sicong Wang, Chen Wei, Yuanhua Feng, Yaoyu Cao, Haiwei Wang, Weiming Cheng, Changsheng Xie, Arata Tsukamoto, Andrei Kirilyuk, Theo Rasing, Alexey V. Kimel and Xiangping Li, All-optical helicity-dependent magnetic switching by first-order azimuthally polarized vortex beams, *Appl. Phys. Lett*., 113, 171108 (2018). https://dx.doi.org/10.1063/1.5051576

Stanciu, C. D., Hansteen, F., Kimel, A. V. and Kirilyuk Tsukamoto, A., All-optical magnetic recording with circularly polarized light, *Phys. Rev. Lett*., 99(4), 047601-047606 (2007). https://dx.doi.org/10.1103/PhysRevLett.99.047601

Udhayakumar, M., Prabakaran, K. and Rajesh, K. B., Generation of ultra-long pure magnetization needle and multiple spots by phase modulated doughnut gaussian beam, *Opt. Laser Technol*., 102, 40-46 (2018b). https://dx.doi.org/10.1016/j.optlastec.2017.12.008

Udhayakumar, M., Prabakaran, K., Rajesh, K. B., Jaroszewicz, Z. and Belafhal, A., Generating Sub wavelength pure longitudinal magnetization probe and chain using complex phase plate, *Opt. Commu*n., 407, 275–279,(2018a). https://dx.doi.org/10.1016/j.optcom.2017.09.007

Van der Ziel, J. P., Peter S. Pershan and Malmstrom, L. D., Optically-induced magnetization resulting from the inverse Faraday effect, *Phys. Rev. Lett*., 15(5), 190–193 (1965). https://dx.doi.org/10.1103/PhysRevLett.15.190

Vetsch, V., Reitz, D., Sague, G., Schmidt, R., Dawkin, S. T. and Rauschenbeutel, A., Optical interface created by laser-cooled atoms trapped in the evanescent field surrounding an optical nanofiber, *Phys. Rev. Lett.*, 104(20), 203603 (2010). https://dx.doi.org/10.1103/PhysRevLett.104.203603

Volkov, P. V. and Novikov, M. A., Inverse Faraday Effect in anisotropic media, *Crystallography Rep*., 47(5), 824–828 (2002). https://dx.doi.org/10.1134/1.1509399

Wang, S., Li, X., Zhou, J. and Gu, M., Ultra long pure longitudinal magnetization needle induced by annular vortex binary optics, *Opt. Lett*., 39(17), 5022–5025 (2014). https://dx.doi.org/10.1364/OL.39.005022

Xiaoyu Weng, Xiumin Gao, Hanming Guo and Songlin Zhuang, Creation of tunable multiple 3D dark spots with cylindrical vector beam, *Appl. Opt.*, 53(11), 2470-2476 (2014). https://dx.doi.org/10.1364/AO.53.002470

Yan, W., Nie, Z., Zhang, X., Wang, Y. and Song, Y., Magnetization shaping generated by tight focusing of azimuthally polarized vortex multi-Gaussian beam, *Appl. Opt*., 56(7), 1940–1946 (2017). https://dx.doi.org/10.1364/AO.56.001940

Yan, W., Nie, Z., Zhang, X., Wang, Y. and Song, Y., Generation of an ultra-long pure longitudinal magnetization needle with high axial homogeneity using an azimuthally polarized beam modulated by pure multi-zone plate phase filter, *J. Opt*., 19(8), 085401 (2017a). https://dx.doi.org/10.1088/2040-8986/aa73ce

Yan, W., Nie, Z., Zhang, X., Wang, Y. and Song, Y., Theoretical guideline for generation of an ultra-long magnetization needle and a super-long conveyed spherical magnetization chain, *Opt. Express*, 25(19), 22268-22279(2017b). https://dx.doi.org/10.1364/OE.25.022268

Zijlstra, P., Chon, J. W. and Gu, M., Five-dimensional optical recording mediated by surface Plasmon's in gold Nano rods, *Nature*, 459(7245), 410-413(2009). https://dx.doi.org/10.1038/nature08053.